LUND UNIVERSITY

Scattering of transient electromagnetic waves in reciprocal bi-isotropic media

Kristensson, Gerhard; Rikte, Sten

1991

[Link to publication](#)

Scattering of transient electromagnetic waves in reciprocal bi-isotropic media

Gerhard Kristensson and Sten Rikte

Gerhard Kristensson
Sten Rikte

Department of Electromagnetic Theory
Lund Institute of Technology
P.O. Box 118
SE-221 00 Lund
Sweden

Abstract

In this paper propagation of transient electromagnetic waves in a reciprocal bi-isotropic medium is presented. The constitutive relations are convolution integrals with two susceptibility kernels that model the medium. The propagation problem is solved by the introduction of a wave-splitting technique. This wave-splitting is used to solve the propagation problem using either an imbedding approach or a Green function technique. In particular, the scattering problem of an electromagnetic wave that impinges normally on a slab of finite or infinite extent is solved. The slab is assumed to be inhomogeneous with respect to depth. The scattering problem consists of finding the reflected and the transmitted fields and the generic quantities are the reflection and the transmission kernels of the medium. Explicit expressions for the rotation and the attenuation of the wave front is presented for the inhomogeneous slab. In the special case of a homogeneous infinite slab it is proved that the reflection kernel satisfies a non-linear Volterra equation of the second kind, very suitable for numerical calculations. It is also proved that no cross polarization contribution appears for the homogeneous slab. Several numerical computations illustrate the analysis.

1   Introduction

In recent years there has been a reborn interest in wave propagation in complex media. Special attention has been paid to wave propagation in bi-isotropic media or more generally bi-anisotropic media. Depending on the symmetry of the medium, whether it is isotropic, reciprocal or lossless, several names for these media are suggested, e.g., magneto-electric, chiral, see Ref. [13] for further details on the nomenclature.

Most contributions in the literature on the wave propagation in bi-isotropic media analyze the problem at fixed frequency. Some of the recent progress in this area is excellently reviewed in [3] and [12]. The transient response of a bi-isotropic medium has recently been addressed and the Kramers-Kronig relations for bi-isotropic media has been derived [4]. However, the wave propagation problem of the transient fields in such media was not analysed. To efficiently cope with the specific problems appearing in transient electromagnetic field propagation more suited methods, that do not rely on a fix frequency formulation, have to be applied.

The present paper utilizes a time domain formulation to analyze the wave propagation problem in a reciprocal bi-isotropic media. Due to the fact that in a time domain formulation all media show dissipative effects, in one form or another, the neutral name bi-isotropic media is used in the present paper.

The emphasis in this paper is on the direct scattering problem and both the reflection and transmission scattering problems are considered. The direct scattering problem is to compute the scattered fields from known material parameters. In the inverse problem, however, the material parameters of the medium are found from scattering data. The inverse scattering problem is addressed in a subsequent paper.

2 Basic equations

During the last decade several papers have shown the applicability of modeling dispersion in a medium with a time convolution in the constitutive relations, see e.g. [1, 7]. This model is extended in this paper to also accommodate bi-isotropic effects, see Ref. [5].

The direct and inverse scattering problems in the dispersive case were first formulated by [1]. The present paper is a generalization of this formulation with respect to bi-isotropy.

The constitutive relations used in this paper model the dispersion of the medium with time convolution integrals.

$$\begin{cases} \boldsymbol{D}(\boldsymbol{r}, t) = \epsilon_0 \left\{ \boldsymbol{E}(\boldsymbol{r}, t) + (G * \boldsymbol{E})(\boldsymbol{r}, t) + c(K * \boldsymbol{B})(\boldsymbol{r}, t) \right\} \\ \boldsymbol{H}(\boldsymbol{r}, t) = \epsilon_0 \left\{ c(K * \boldsymbol{E})(\boldsymbol{r}, t) + c^2 \boldsymbol{B}(\boldsymbol{r}, t) \right\} \end{cases} \tag{2.1}$$

where time convolution is denoted by a $*$, i.e.,

$$(G * \boldsymbol{E})(\boldsymbol{r}, t) = \int_{-\infty}^{t} G(\boldsymbol{r}, t - t') \boldsymbol{E}(\boldsymbol{r}, t') \, dt'$$

and where $c = 1/\sqrt{\epsilon_0 \mu_0}$ is the speed of light in vacuum. Besides the isotropy, the form of the constitutive relations implies that the medium is reciprocal. These assumptions motivate constitutive relations like the ones found above in (2.1). The mathematical background behind these assumptions is given in [5].

The two susceptibility kernels, $G(\boldsymbol{r}, t)$ and $K(\boldsymbol{r}, t)$, are in the general case functions of both the spatial variables $\boldsymbol{r}$ and the time variable t. In the medium they are assumed to be continuously differentiable in the time variable t for $t > 0$ as well as in the spatial variables $\boldsymbol{r}$. Causality implies that $G(\boldsymbol{r}, t)$ and $K(\boldsymbol{r}, t)$ are zero for negative time t. Some of the results presented in this paper hold only for the homogeneous case when there is no spatial variation of the two susceptibility kernels $G(\boldsymbol{r}, t)$ and $K(\boldsymbol{r}, t)$. The results that hold only for the homogeneous case will be pointed out explicitly and these results are collected in a separate section.

The susceptibility kernel $G(\boldsymbol{r}, t)$ models the usual dispersion in the medium. The other susceptibility kernel $K(\boldsymbol{r}, t)$, however, models the bi-isotropic effects. This kernel gives the coupling effects between the electric and the magnetic fields that are characteristic for a bi-isotropic medium.

It is straightforward to show, from (2.1) and the Maxwell equations, that the electric field $\boldsymbol{E}$ satisfies

$$\nabla \times (\nabla \times \boldsymbol{E}) = -\frac{1}{c^2} \partial_t^2 \left\{ \boldsymbol{E} + G * \boldsymbol{E} \right\} + \frac{1}{c} \partial_t \left\{ K * (\nabla \times \boldsymbol{E}) \right\}$$
$$+ \frac{1}{c} \partial_t \nabla \times (K * \boldsymbol{E})$$

$$G(z,t) = 0 \qquad G(z,t) \neq 0 \qquad G(z,t) = 0$$
$$K(z,t) = 0 \qquad K(z,t) \neq 0 \qquad K(z,t) = 0$$
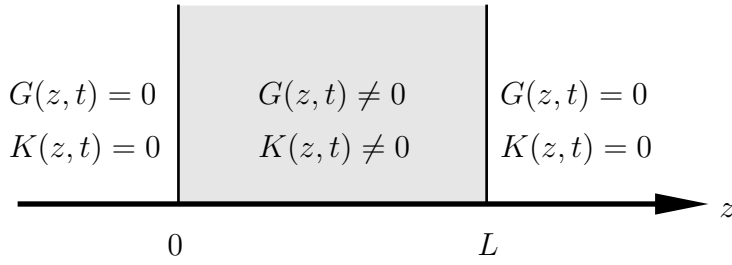
Figure 1: Geometry of the problem.

In this paper the medium is assumed to vary only with depth z of the medium, see Figure 1. Thus, the susceptibility kernels $G(\boldsymbol{r},t)$ and $K(\boldsymbol{r},t)$ are functions of depth z and time t only. Furthermore, the electromagnetic field is assumed to be transversely polarized and to depend only on the spatial variable z and time t, i.e.,

$$\boldsymbol{E}(\boldsymbol{r},t) = \boldsymbol{E}(z,t) = \hat{x}_1 E_1(z,t) + \hat{x}_2 E_2(z,t)$$

where $\hat{x}_1$ and $\hat{x}_2$ are two unit vectors in the transverse directions. The wave equation then simplifies to

$$\partial_z^2 \boldsymbol{E}(z,t) = \frac{1}{c^2} \left\{ \partial_t^2 \boldsymbol{E}(z,t) + (\mathbf{G} * \partial_t^2 \boldsymbol{E})(z,t) \right\}$$
$$- \frac{2}{c}(\mathbf{K} * \partial_t \partial_z \boldsymbol{E})(z,t) - \frac{1}{c}(\partial_z \mathbf{K} * \partial_t \boldsymbol{E})(z,t) \tag{2.2}$$

where the 2×2 operators $\mathbf{G}(z,t)$ and $\mathbf{K}(z,t)$ are defined as

$$\mathbf{G}(z,t) = \begin{pmatrix} G(z,t) & 0 \\ 0 & G(z,t) \end{pmatrix}, \qquad \mathbf{K}(z,t) = \begin{pmatrix} 0 & -K(z,t) \\ K(z,t) & 0 \end{pmatrix} \tag{2.3}$$

and where matrix multiplication is used in the convolutions in (2.2), i.e.,

$$(\mathbf{G} * \boldsymbol{E})(\boldsymbol{r},t) = \sum_{i,j=1}^{2} \hat{x}_i \int_{-\infty}^{t} G_{ij}(\boldsymbol{r},t-t') E_j(\boldsymbol{r},t') \, dt'$$

and similarly for convolution with $\mathbf{K}$. Throughout this paper vectors are denoted by slanted boldface and matrices in upright boldface. Notice that the matrices $\mathbf{G}(z,t)$ and $\mathbf{K}(z,t)$ commute.

The wave equation in (2.2) can be rewritten as a system of first order equations.

$$\partial_z \begin{pmatrix} \boldsymbol{E} \\ \partial_z \boldsymbol{E} \end{pmatrix} = \begin{pmatrix} \mathbf{0} & \mathbf{I} \\ \frac{1}{c^2}\left\{\mathbf{I}\partial_t^2 + \mathbf{G} * (\partial_t^2 \cdot)\right\} - \frac{1}{c}\partial_z \mathbf{K} * (\partial_t \cdot) & -\frac{2}{c}\mathbf{K} * (\partial_t \cdot) \end{pmatrix} \begin{pmatrix} \boldsymbol{E} \\ \partial_z \boldsymbol{E} \end{pmatrix}$$
$$= \mathcal{D} \begin{pmatrix} \boldsymbol{E} \\ \partial_z \boldsymbol{E} \end{pmatrix} \tag{2.4}$$

where $\mathbf{I}$ is the 2×2 identity matrix operator and $\mathbf{0}$ is the 2×2 zero matrix operator.

3 Wave splitting

In this section the wave splitting used in this paper is presented. This splitting is identical to the splitting used in, e.g., Beezley and Krueger [1] and later also Kristensson [7].

The splitting is mathematically a change in the dependent variables and it is defined as

$$\boldsymbol{E}^{\pm}(z,t) = \frac{1}{2}\left\{ \boldsymbol{E}(z,t) \mp c\partial_t^{-1}\partial_z \boldsymbol{E}(z,t) \right\} \tag{3.1}$$

where $\partial_t^{-1}f(z,t) = \int_{-\infty}^{t} f(z,t')\,dt'$. In free space, where $\mathbf{G} = \mathbf{K} = \mathbf{0}$, it is easy to see that $\boldsymbol{E}^+$ and $\boldsymbol{E}^-$ are right and left traveling waves, respectively, i.e.,

$$\boldsymbol{E}^+(z,t) = \boldsymbol{f}(t - z/c)$$
$$\boldsymbol{E}^-(z,t) = \boldsymbol{g}(t + z/c)$$

The transformation in (3.1) is, however, well-defined also for points inside the medium even though no right or left moving waves can be identified. Figure 2 gives a formal picture of the wave splitting for such a point z inside the medium.
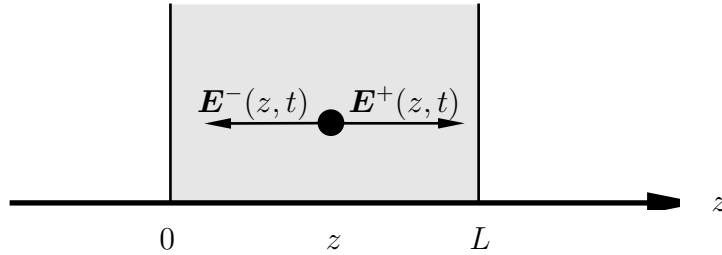

Figure 2: The wave splitting.

In a matrix notation this wave splitting, defined by (3.1), is

$$\begin{pmatrix} \boldsymbol{E}^+(z,t) \\ \boldsymbol{E}^-(z,t) \end{pmatrix} = \frac{1}{2}\begin{pmatrix} \mathbf{I} & -c\partial_t^{-1}\mathbf{I} \\ \mathbf{I} & c\partial_t^{-1}\mathbf{I} \end{pmatrix}\begin{pmatrix} \boldsymbol{E}(z,t) \\ \partial_z\boldsymbol{E}(z,t) \end{pmatrix} = \mathcal{P}\begin{pmatrix} \boldsymbol{E}(z,t) \\ \partial_z\boldsymbol{E}(z,t) \end{pmatrix}$$

The formal inverse of the operator $\mathcal{P}$ is

$$\mathcal{P}^{-1} = \begin{pmatrix} \mathbf{I} & \mathbf{I} \\ -\frac{1}{c}\partial_t\mathbf{I} & \frac{1}{c}\partial_t\mathbf{I} \end{pmatrix}$$

The partial differential equation that the plus and minus fields defined above satisfies can be found from the wave equation (2.4) and the definition of the wave splitting in (3.1). The result is

$$\partial_z\begin{pmatrix} \boldsymbol{E}^+ \\ \boldsymbol{E}^- \end{pmatrix} = \mathcal{P}\mathcal{D}\mathcal{P}^{-1}\begin{pmatrix} \boldsymbol{E}^+ \\ \boldsymbol{E}^- \end{pmatrix} = \begin{pmatrix} -\frac{1}{c}\partial_t\mathbf{I} - \boldsymbol{\alpha} - \boldsymbol{\beta} & -\boldsymbol{\alpha} + \boldsymbol{\beta} \\ \boldsymbol{\alpha} + \boldsymbol{\beta} & \frac{1}{c}\partial_t\mathbf{I} + \boldsymbol{\alpha} - \boldsymbol{\beta} \end{pmatrix}\begin{pmatrix} \boldsymbol{E}^+ \\ \boldsymbol{E}^- \end{pmatrix} \tag{3.2}$$

where

$$\begin{cases} \boldsymbol{\alpha} = \dfrac{1}{2c}\mathbf{G} * (\partial_t \cdot) - \dfrac{1}{2}\partial_z \mathbf{K} * (\cdot) \\ \boldsymbol{\beta} = \dfrac{1}{c}\mathbf{K} * (\partial_t \cdot) \end{cases}$$

This PDE is equivalent to the wave equation (2.4) or (2.2).

Any finite jump discontinuity in the field $\boldsymbol{E}^+$ at $z = 0$ will propagate through the medium and at a point z inside the medium the field has attenuated and rotated. The jump discontinuity in the field $\boldsymbol{E}^+$ can be obtained by propagation of singularity arguments. The result is

$$\left[\boldsymbol{E}^+(z, t + z/c)\right] = \mathbf{Q}(z)\left[\boldsymbol{E}^+(0, t)\right]$$

where the 2×2 matrix $\mathbf{Q}(z)$ gives the rotation and the attenuation of the wave front as it propagates through the medium. The square bracket $\left[\boldsymbol{E}^+(z, t + z/c)\right]$ denotes the jump discontinuity of the field at the point $(z, t + z/c)$. The field $\boldsymbol{E}^-$ shows no jump discontinuity of this kind and therefore the total field $\boldsymbol{E}$ has exactly the same jump discontinuity as the field $\boldsymbol{E}^+$ above. The jump discontinuity $\left[\boldsymbol{E}^+(0, t)\right]$ is the same on either side of the interface of the slab. This is easily seen from the boundary conditions which are analysed in Section 5.

The matrix $\mathbf{Q}(z)$ satisfies the following first order differential equation found by use of propagation of singularity arguments.

$$\begin{aligned} \frac{d}{dz}\mathbf{Q}(z) &= -\frac{1}{2c}\left(\mathbf{G}(z, 0) + 2\mathbf{K}(z, 0)\right)\mathbf{Q}(z) \\ \mathbf{Q}(0) &= \mathbf{I} \end{aligned} \tag{3.3}$$

This matrix equation can be explicitly solved and the general solution is $\mathbf{Q}(z) = \mathbf{Q}(0, z)$, where

$$\mathbf{Q}(z_1, z_2) = e^{-\frac{1}{2c}\int_{z_1}^{z_2} G(z', 0)\, dz'}\begin{pmatrix} \cos\phi(z_1, z_2) & -\sin\phi(z_1, z_2) \\ \sin\phi(z_1, z_2) & \cos\phi(z_1, z_2) \end{pmatrix} \tag{3.4}$$

where the angle of rotation of the wave front $\phi(z_1, z_2)$ is

$$\phi(z_1, z_2) = -\frac{1}{c}\int_{z_1}^{z_2} K(z', 0)\, dz' \tag{3.5}$$

Notice that this result holds for an inhomogeneous slab with arbitrary susceptibility kernels $G(z, t)$ and $K(z, t)$. This result corroborates the rotation of the plane of polarization and the attenuation of the wave front in the high frequency limit in a homogeneous medium [6]. The form of the matrix $\mathbf{Q}$ implies that $\mathbf{Q}$ commutes with $\mathbf{G}$ and $\mathbf{K}$.

4 Imbedding equations

The scattering problem of transient electromagnetic waves is now addressed. The approach that is presented in this section is based upon an imbedding procedure. This technique has been applied to several related problems of similar nature, e.g, dissipative inhomogeneous lossy slab [8–11] and dissipative medium [1, 7].
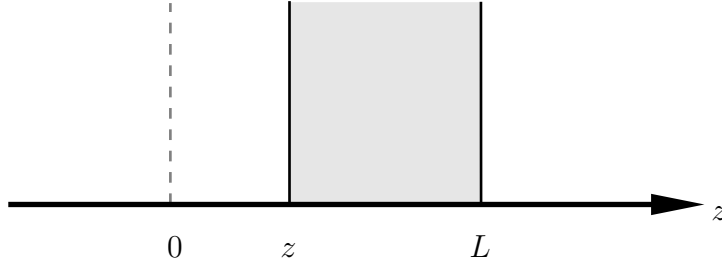

Figure 3: The imbedding geometry.

Consider a subsection $[z, L]$ of the original physical slab $[0, L]$, see also Figure 3. From Duhamel's principle [2], it can be shown that there exists a linear relation between the plus and the minus fields, $\boldsymbol{E}^{\pm}(z, t)$, at z and similarly between the plus fields at L and z. These relations are the imbedding reflection and transmission operators. The explicit form of these operators is

$$\boldsymbol{E}^{-}(z, t) = \int_{-\infty}^{t} \mathbf{R}(z, t - t')\boldsymbol{E}^{+}(z, t') \, dt' \tag{4.1}$$

$$\boldsymbol{E}^{+}(L, t + (L - z)/c) = \mathbf{Q}(z, L) \left\{ \boldsymbol{E}^{+}(z, t) + \int_{-\infty}^{t} \mathbf{T}(z, t - t')\boldsymbol{E}^{+}(z, t') \, dt' \right\} \tag{4.2}$$

where the matrices $\mathbf{R}$ and $\mathbf{T}$ due to the axial symmetry are:

$$\mathbf{R}(z, t) = \begin{pmatrix} R_1(z, t) & -R_2(z, t) \\ R_2(z, t) & R_1(z, t) \end{pmatrix} \tag{4.3}$$

$$\mathbf{T}(z, t) = \begin{pmatrix} T_1(z, t) & -T_2(z, t) \\ T_2(z, t) & T_1(z, t) \end{pmatrix} \tag{4.4}$$

and where the matrix $\mathbf{Q}(z, L)$ that gives the attenuation and the rotation of the wave front is given by (3.4) and (3.5). Note that the matrices $\mathbf{R}$ and $\mathbf{T}$ commute with $\mathbf{G}$ and $\mathbf{K}$ and with $\mathbf{Q}$ and, furthermore, that the kernels R_i and T_i are zero for negative time t.

The kernels $R_i, i = 1, 2$ and $T_i, i = 1, 2$ are referred to as the reflection and transmission imbedding kernels, respectively, for a subsection $[z, L]$ of the physical medium $[0, L]$. These kernels are the generic quantities of the scattering problem and independent of the excitation of the slab. The component R_1 gives the co-polarized contribution to the reflection, whereas R_2 gives the cross-polarized contribution. Note that these kernels are not the physical reflection kernels. They are, however, naturally and easily related to the physical kernels. The relation between the imbedding kernels and the physical kernels is presented in Section 5.

Analogous to the dispersive case [1], the reflection imbedding kernels R_1 and R_2 satisfy integro-differential equations. These equations and the corresponding boundary condition are straightforward to find using (4.1) and (3.2). The result is $(t > 0)$

$$2c\partial_z \mathbf{R} - 4\partial_t \mathbf{R} = \partial_t \{\mathbf{G} + 2\mathbf{K} + \mathbf{G} * [2\mathbf{R} + \mathbf{R} * \mathbf{R}] - 2\mathbf{K} * \mathbf{R} * \mathbf{R}\}$$
$$- c\{\partial_z \mathbf{K} + \partial_z \mathbf{K} * [2\mathbf{R} + \mathbf{R} * \mathbf{R}]\} \tag{4.5}$$

$$\mathbf{R}(z,0) = -\frac{1}{4}\mathbf{G}(z,0) - \frac{1}{2}\mathbf{K}(z,0) \tag{4.6}$$

where the argument zero means time $t = 0^+$, i.e., $\mathbf{R}(z,0) = \mathbf{R}(z,0^+)$. The derivation of these equations uses the fact that the operators $\mathbf{G}$ and $\mathbf{K}$ and $\mathbf{R}$ all commute.

At one round trip, $t = 2(L-z)/c$, there is a finite jump discontinuity in the reflection operator $\mathbf{R}$. This jump discontinuity can be determined from (4.5) by propagation of singularity arguments and the use of (5.3). The explicit result is

$$[\mathbf{R}(z,t)]_{t=\frac{2(L-z)}{c}-0}^{t=\frac{2(L-z)}{c}+0} = \frac{1}{4}e^{-\int_z^L \frac{G(z',0)}{c} dz'}\mathbf{G}(L,0) \tag{4.7}$$

This implies that there is no jump discontinuity in R_2 at one round trip, and the jump discontinuity in R_1 is identical to the corresponding one for a pure dispersive medium [7].

In complete analogy to the analysis above for the imbedding kernel $\mathbf{R}(z,t)$, the imbedding kernel $\mathbf{T}(z,t)$ satisfies an imbedding equation. This equation is

$$2c\partial_z \mathbf{T} = -\{\mathbf{G}(z,0) + 2\mathbf{K}(z,0)\}\mathbf{T} - c\{\partial_z \mathbf{K} + \partial_z \mathbf{K} * [\mathbf{R} + \mathbf{T} + \mathbf{R} * \mathbf{T}]\}$$
$$+ \partial_t \{\mathbf{G} + 2\mathbf{K} + [\mathbf{G} + 2\mathbf{K}] * \mathbf{T} + [\mathbf{G} - 2\mathbf{K}] * [\mathbf{R} + \mathbf{R} * \mathbf{T}]\} \tag{4.8}$$

$$\mathbf{T}(L,t) = \mathbf{0}$$

The boundary condition for $\mathbf{T}$ at $z = L$ is determined by (4.2). The value of the transmission imbedding kernel at $t = 0$ can be evaluated analytically from (4.8). This result is

$$\mathbf{T}(z,0) = \frac{1}{2}\left(\mathbf{K}(L,0) - \mathbf{K}(z,0)\right) + \int_z^L \mathbf{A}(z')\,dz'$$

where the 2×2 matrix $\mathbf{A}(z)$ is

$$\mathbf{A}(z) = -\frac{1}{2c}\left(\mathbf{G}'(z,0) + 2\mathbf{K}'(z,0)\right) + \frac{1}{8c}\left(\mathbf{G}(z,0)\mathbf{G}(z,0) - 4\mathbf{K}(z,0)\mathbf{K}(z,0)\right) \tag{4.9}$$

where $\mathbf{G}'(z,0) = \partial_t \mathbf{G}(z,0)$ and similarly for $\mathbf{K}'(z,0)$.

For a homogeneous slab the integral can be evaluated explicitly.

$$\mathbf{T}(z,0) = -(L-z)\left\{\frac{1}{2c}\left(\mathbf{G}'(0) + 2\mathbf{K}'(0)\right) - \frac{1}{8c}\left(\mathbf{G}(0)\mathbf{G}(0) - 4\mathbf{K}(0)\mathbf{K}(0)\right)\right\}$$

In the ordinary dispersive case, $K(t) = 0$, the imbedding equations (4.5) and (4.8) simplify to the ones given in Ref. [1]. The imbedding equations, (4.5) and (4.8), can be solved numerically to find the imbedding kernels $\mathbf{R}(0,t)$ and $\mathbf{T}(0,t)$. In the next section the relation between these imbedding kernels and the physical ones are analysed. That relation constitutes the final step to compute the physical scattering kernels of the problem.

5 Boundary conditions and the physical reflection and transmission kernels

The imbedding kernels $\mathbf{R}$ and $\mathbf{T}$ in Section 4 have to be related to the scattering kernels measured in an experimental setup. This is analysed in this section.

The reflected field $\boldsymbol{E}^r(t)$ (measured at $z = 0$ to the left of the slab) is related to the incident field $\boldsymbol{E}^i(t)$ (measured at $z = 0$ to the left of the slab) by the physical reflection kernel $\mathcal{R}(t)$. The transmitted field $\boldsymbol{E}^t(t)$ (measured at $z = L$ to the right of the slab) is related to the incident field $\boldsymbol{E}^i(t)$ by the physical transmission kernel $\mathcal{T}(t)$. These kernels are the generic quantities for the scattering problem and independent of the excitation $\boldsymbol{E}^i(t)$ and related to the imbedding kernels $\mathbf{R}$ and $\mathbf{T}$. The relation between the physical fields and the physical kernels are

$$\boldsymbol{E}^r(t) = \int_{-\infty}^{t} \mathcal{R}(t - t')\boldsymbol{E}^i(t')\, dt'$$

$$\boldsymbol{E}^t(L, t + L/c) = \mathbf{Q}(L) \left\{ \boldsymbol{E}^i(t) + \int_{-\infty}^{t} \mathcal{T}(t - t')\boldsymbol{E}^i(t')\, dt' \right\}$$

where the physical kernels $\mathcal{R}$ and $\mathcal{T}$ have the same form as (4.3) and (4.4), respectively, i.e.,

$$\mathcal{R}(t) = \begin{pmatrix} R_{\text{co}}(t) & -R_{\text{cross}}(t) \\ R_{\text{cross}}(t) & R_{\text{co}}(t) \end{pmatrix}$$

$$\mathcal{T}(t) = \begin{pmatrix} T_{\text{co}}(t) & -T_{\text{cross}}(t) \\ T_{\text{cross}}(t) & T_{\text{co}}(t) \end{pmatrix}$$

The rotation matrix $\mathbf{Q}(L) = \mathbf{Q}(0, L)$, explicitly given by (3.4) and (3.5), determines the rotation and the attenuation of the wave front of the transmitted field.

The boundary conditions at the interface of the slab at $z = 0$ and at $z = L$ are continuity of the tangential electric and magnetic fields, respectively. In terms of the field $\boldsymbol{E}(z, t)$ the boundary conditions are

$$\left. \begin{array}{l} \boldsymbol{E} \\ K * \boldsymbol{E} + c\partial_t^{-1}\partial_z \begin{pmatrix} 0 & 1 \\ -1 & 0 \end{pmatrix} \boldsymbol{E} \end{array} \right\} \quad \text{continuous at } z = 0 \text{ and } z = L$$

From these expressions it is straightforward to derive the boundary conditions for the fields $\boldsymbol{E}^+$ and $\boldsymbol{E}^-$. The result is

$$\left. \begin{array}{l} \boldsymbol{E}^+ + \boldsymbol{E}^- \\ \mathbf{K} * \boldsymbol{E}^+ - \boldsymbol{E}^+ + \mathbf{K} * \boldsymbol{E}^- + \boldsymbol{E}^- \end{array} \right\} \quad \text{continuous at } z = 0 \text{ and } z = L \qquad (5.1)$$

The boundary conditions at $z = 0$ imply that the physical kernel $\mathcal{R}$ is related to the imbedding kernel $\mathbf{R}(0, t)$ by a system of Volterra equations of the second kind.

$$\mathcal{R}(t) - \frac{1}{2}\left(\mathbf{K}(0, \cdot) * \mathcal{R}\right)(t) - \frac{1}{2}\left(\mathbf{K}(0, \cdot) * \mathcal{R} * \mathbf{R}(0, \cdot)\right)(t)$$

$$= \mathbf{R}(0, t) + \frac{1}{2}\mathbf{K}(0, t) + \frac{1}{2}\left(\mathbf{K}(0, \cdot) * \mathbf{R}(0, \cdot)\right)(t)$$

Notice that this equation is a Volterra equation of the second kind in either $\mathcal{R}$ ($\mathbf{R}(0,t)$ known) or $\mathbf{R}$ ($\mathcal{R}(t)$ known). The first problem is the one relevant to the solution of the direct problem. The latter one gives the imbedding kernels $\mathbf{R}(0,t)$ in terms of the physical kernel $\mathcal{R}$ and is more appropriate for the solution of the inverse problem. In both cases they are easy to compute numerically. It is convenient to write this in terms of the appropriate resolvent kernel. Let the matrix resolvent $\mathbf{L}$ be defined by

$$\mathbf{L} - \mathbf{L} * \mathbf{X} = \mathbf{X}$$

where

$$\mathbf{X} = \frac{1}{2}\mathbf{K}(0,t) + \frac{1}{2}\left(\mathbf{K}(0,\cdot) * \mathbf{R}(0,\cdot)\right)(t)$$

Then the reflection kernel $\mathcal{R}$ is determined by

$$\mathcal{R} = \mathbf{R} + \mathbf{L} + \mathbf{L} * \mathbf{R}$$

The reflection kernel $\mathbf{R}(0,t)$ can likewise be expressed in $\mathcal{R}(t)$ by a resolvent kernel. The result is

$$\mathbf{R} = \mathcal{R} - \mathbf{M} - \mathbf{M} * \mathcal{R} \tag{5.2}$$

where the matrix resolvent $\mathbf{M}$ is defined by

$$\mathbf{M} + \mathbf{M} * \mathbf{Y} = \mathbf{Y}$$

where

$$\mathbf{Y} = \frac{1}{2}\mathbf{K}(0,t) + \frac{1}{2}\left(\mathbf{K}(0,\cdot) * \mathcal{R}\right)(t)$$

The jump discontinuity in $\mathcal{R}(t)$ at $t = L/c$ is the same as the jump in $\mathbf{R}(0,t)$ given by (4.7), i.e.

$$\left[\mathcal{R}(t)\right]_{t=\frac{2L}{c}-0}^{t=\frac{2L}{c}+0} = \frac{1}{4}e^{-\int_0^L \frac{G(z,0)}{c}\,dz}\mathbf{G}(L,0)$$

The boundary conditions in (5.1) at $z = L$ give the appropriate boundary value for the imbedding kernel $\mathbf{R}$ at $z = L$. The result is

$$\mathbf{R}(L,t) + \frac{1}{2}\mathbf{K}(L,t) + \frac{1}{2}\left(\mathbf{K}(L,\cdot) * \mathbf{R}(L,\cdot)\right)(t) = \mathbf{0} \tag{5.3}$$

The connection between the physical kernel $\mathcal{T}(t)$ and the imbedding kernel $\mathbf{T}(0,t)$ is also determined by (5.1). This result is found by a similar analysis as the one presented above, and this result is

$$\mathcal{T}(t) + \frac{1}{2}\left(\mathbf{K}(L,\cdot) * \mathcal{T}\right)(t) = \frac{1}{2}\mathbf{K}(0,t) - \frac{1}{2}\mathbf{K}(L,t) + \mathbf{T}(0,t)$$
$$+ \frac{1}{2}\left(\mathbf{K}(0,\cdot) * [\mathcal{R} + \mathbf{T}(0,\cdot) + \mathcal{R} * \mathbf{T}(0,\cdot)]\right)(t)$$

This equation relates the physical kernel $\mathcal{T}$ to the imbedding kernel $\mathbf{T}(0,t)$. Notice that this equation is a Volterra equation of the second kind (in either $\mathcal{T}$ or $\mathbf{T}$) and therefore easy to solve numerically.
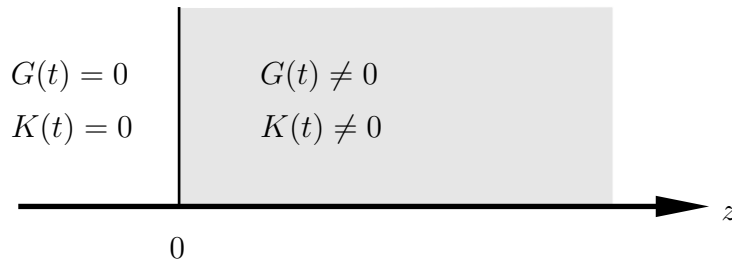
6 Homogeneous, semi-infinite slab

Figure 4: Geometry of the semi-infinite slab problem.

If the medium is homogeneous and semi-infinite several simplifications occur. In this section these special results are collected.

In a homogeneous and semi-infinite medium, see Figure 4, the reflection kernels R_1 and R_2 are independent of the spatial coordinate z. The imbedding equation (4.5) can then be integrated with respect to time using equation (4.6). The result is

$$4\mathbf{R} + \mathbf{G} + 2\mathbf{K} + \mathbf{G} * [2\mathbf{R} + \mathbf{R} * \mathbf{R}] - 2\mathbf{K} * \mathbf{R} * \mathbf{R} = \mathbf{0} \tag{6.1}$$

Notice that this is an integral equation in the time variable without any explicit partial derivatives. The imbedding kernels of $\mathbf{R}$ are independent of z.

The equation (5.2) can now be used to transform (6.1) into an equation for $\mathcal{R}$. The result is

$$4\mathcal{R} + \mathbf{G} + \mathbf{K} * \mathbf{K} + [\mathbf{G} + \mathbf{K} * \mathbf{K}] * [2\mathcal{R} + \mathcal{R} * \mathcal{R}] = \mathbf{0} \tag{6.2}$$

This equation shows that there is no cross-polarized coupling for the semi-infinite homogeneous slab, since $\mathbf{G} + \mathbf{K} * \mathbf{K}$ is a diagonal operator, i.e., the kernel $R_{\mathrm{cross}} = 0$. This is not only true for a homogeneous, semi-infinite case, but for the homogeneous slab of finite extent as can be proved by Laplace transform techniques.

The equation for the co-polarized part of the physical kernel, which is denoted by $R_{\mathrm{co}}(t)$, is

$$G - K * K + 4R_{\mathrm{co}} + (G - K * K) * (2R_{\mathrm{co}} + R_{\mathrm{co}} * R_{\mathrm{co}}) = 0$$

For the direct scattering problem this equation is a nonlinear integral equation for the unknown kernel $R_{\mathrm{co}}(t)$. A direct comparison with the imbedding equation in Ref. [1] shows that the physical reflection kernel for the homogeneous, semi-infinite bi-isotropic slab satisfy the same equation as the dispersive slab when the susceptibility kernel $G(t)$ is replaced with $G(t) - (K * K)(t)$. As a consequence of this observation, at normal incidence the reflection kernel of a homogeneous, semi-infinite bi-isotropic slab is indistinguishable from that of a dispersive medium with a modified susceptibility kernel.

7 The Green functions

In this section an additional way of solving the scattering problem for a bi-isotropic medium in the time domain is presented. This method employs a Green function technique.

The invariant imbedding formulation in Section 4 uses the relation between the field $\boldsymbol{E}^-(z,t)$ and $\boldsymbol{E}^+(z,t)$ at a point z inside the slab, see (4.1). It is also possible to relate the fields $\boldsymbol{E}^-(z,t)$ and $\boldsymbol{E}^+(z,t)$ at a point z inside the slab to the excitation $\boldsymbol{E}^+(0,t)$ at $z = 0^+$. This relation defines the Green functions $\mathbf{G}^\pm(z,t)$.

$$
\begin{aligned}
\boldsymbol{E}^+(z,t+z/c) &= \mathbf{Q}(z) \left\{ \boldsymbol{E}^+(0,t) + \int_{-\infty}^t \mathbf{G}^+(z,t-t')\boldsymbol{E}^+(0,t')\,dt' \right\} \\
\boldsymbol{E}^-(z,t+z/c) &= \mathbf{Q}(z) \int_{-\infty}^t \mathbf{G}^-(z,t-t')\boldsymbol{E}^+(0,t')\,dt'
\end{aligned}
\tag{7.1}
$$

where the 2×2 matrix $\mathbf{Q}(z) = \mathbf{Q}(0,z)$ is given by (3.4) and (3.5), and the two 2×2 Green functions $\mathbf{G}^+(z,t)$ and $\mathbf{G}^-(z,t)$ are defined as

$$
\mathbf{G}^\pm(z,t) = \begin{pmatrix} G_1^\pm(z,t) & -G_2^\pm(z,t) \\ G_2^\pm(z,t) & G_1^\pm(z,t) \end{pmatrix}
$$

The form of the Green functions $\mathbf{G}^\pm$ implies that $\mathbf{G}^\pm$, $\mathbf{Q}$, $\mathbf{G}$, $\mathbf{K}$, $\mathbf{T}$ and $\mathbf{R}$ all commute.
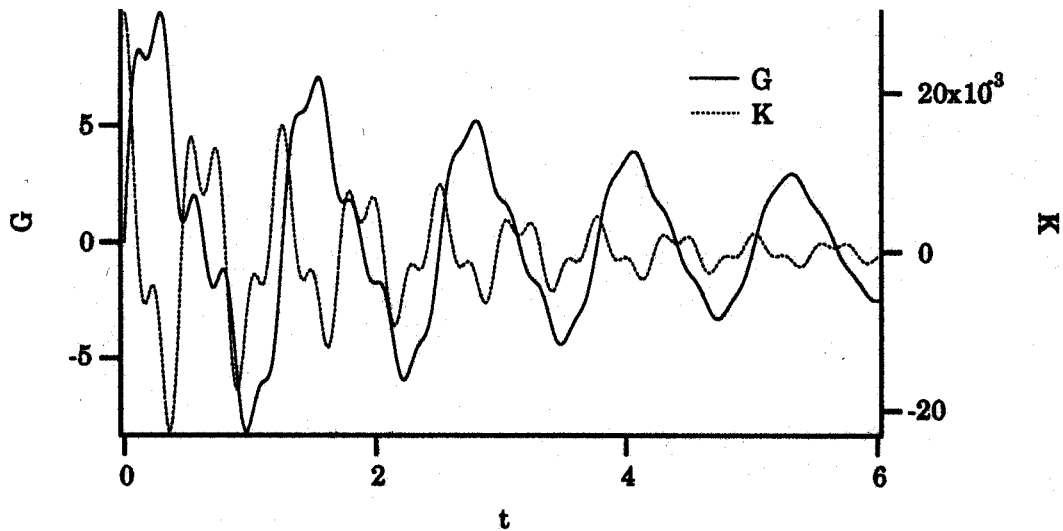

Figure 5: The susceptibility kernels for a multi-frequency Lorentz medium. The time scale is in units of L/c and the amplitude of the kernels in units of c/L.

The definition of $\mathbf{G}^\pm$ given above suggests that there is a connection between the matrix kernels $\mathbf{R}$ and $\mathbf{T}$ and the Green functions $\mathbf{G}^\pm$. This connection is easily

found by repeated use of (7.1), (4.1) and (4.2).

$$\mathbf{G}^+(L,t) = \mathbf{G}^+(z,t) + \mathbf{T}(z,t) + \big(\mathbf{T}(z,\cdot) * \mathbf{G}^+(z,\cdot)\big)(t)$$
$$\mathbf{G}^-(z,t) = \mathbf{R}(z,t) + \big(\mathbf{R}(z,\cdot) * \mathbf{G}^+(z,\cdot)\big)(t) \tag{7.2}$$

The boundary values of the Green functions at $z = 0$ and at $z = L$ are also found from (7.1), (4.1) and (4.2). The explicit values are

$$\mathbf{G}^+(0,t) = \mathbf{0}$$
$$\mathbf{G}^-(0,t) = \mathbf{R}(0,t)$$
$$\mathbf{G}^+(L,t) = \mathbf{T}(0,t)$$

The relation between the Green functions $\mathbf{G}^+(L,t)$ and $\mathbf{G}^-(L,t)$ is found by using (7.2) and (5.3).

$$\mathbf{G}^-(L,t) + \frac{1}{2}\mathbf{K}(L,t) + \frac{1}{2}\big(\mathbf{K}(L,\cdot) * \mathbf{G}^-(L,\cdot)\big)(t) + \frac{1}{2}\big(\mathbf{K}(L,\cdot) * \mathbf{G}^+(L,\cdot)\big)(t) = \mathbf{0}$$
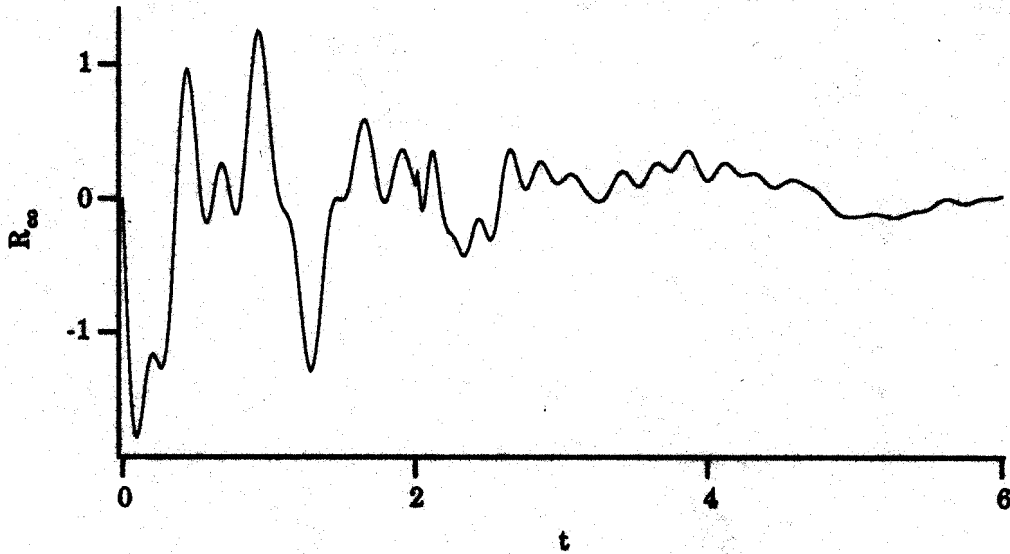

Figure 6: The reflection kernel $R_{\mathrm{co}}(t)$ for the multi-frequency Lorentz medium shown in Figure 5. The time scale is in units of L/c and the amplitude of the kernel in units of c/L.

The imbedding kernels $\mathbf{R}$ and $\mathbf{T}$ satisfy integro-differential equations, see (4.5) and (4.8). The reflection kernel equation was non-linear in $\mathbf{R}$. It is obvious from the coupling between the imbedding kernels and the Green functions $\mathbf{G}^+(z,t)$ and

$\mathbf{G}^-(z, t)$ that the Green functions also satisfy equations. These differential equations are of first order and linear in $\mathbf{G}^\pm$. Their explicit form are

$$2c\partial_z \mathbf{G}^+ = -\partial_t \left\{ (\mathbf{G} + 2\mathbf{K}) + \mathbf{G} * (\mathbf{G}^+ + \mathbf{G}^-) + 2\mathbf{K} * (\mathbf{G}^+ - \mathbf{G}^-) \right\}$$
$$+ \{ \mathbf{G}(z, 0) + 2\mathbf{K}(z, 0) \} \mathbf{G}^+ \tag{7.3}$$
$$+ c \{ \partial_z \mathbf{K} + (\partial_z \mathbf{K}) * (\mathbf{G}^+ + \mathbf{G}^-) \}$$

$$2c\partial_z \mathbf{G}^- - 4\partial_t \mathbf{G}^- = \partial_t \left\{ (\mathbf{G} + 2\mathbf{K}) + \mathbf{G} * (\mathbf{G}^+ + \mathbf{G}^-) + 2\mathbf{K} * (\mathbf{G}^+ - \mathbf{G}^-) \right\}$$
$$+ \{ \mathbf{G}(z, 0) + 2\mathbf{K}(z, 0) \} \mathbf{G}^- \tag{7.4}$$
$$- c \{ \partial_z \mathbf{K} + (\partial_z \mathbf{K}) * (\mathbf{G}^+ + \mathbf{G}^-) \}$$

and at $t = 0^+$

$$\mathbf{G}^-(z, 0) = -\frac{1}{4} (\mathbf{G}(z, 0) + 2\mathbf{K}(z, 0))$$

These equations degenerate to the simple dispersive case, see Ref. [7], as $K(t)$ vanishes.
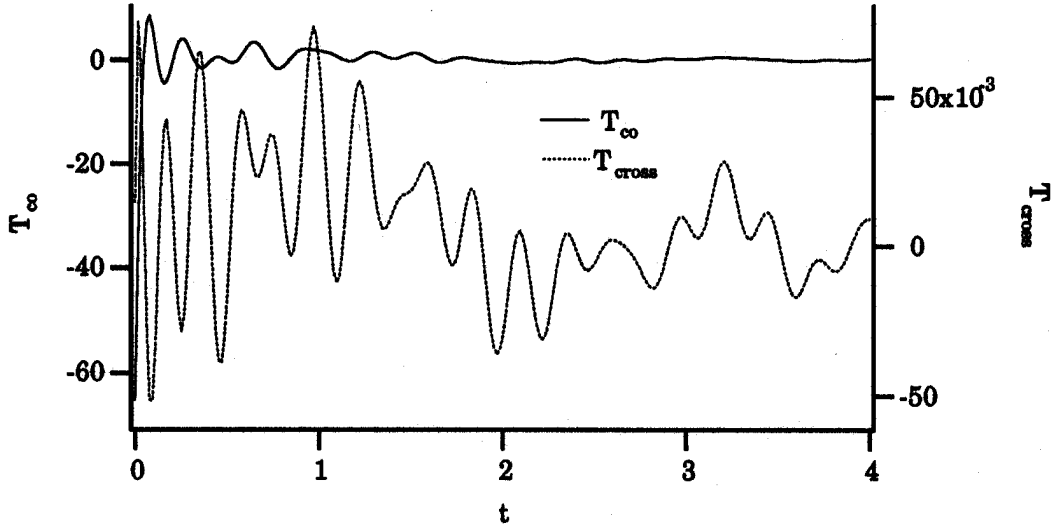

Figure 7: The transmission kernels $T_{\mathrm{co}}(t)$ and $T_{\mathrm{cross}}(t)$ for the multi-frequency Lorentz medium shown in Figure 5. The time scale is in units of L/c and the amplitude of the kernel in units of c/L.

Furthermore, there are finite jump discontinuities in the Green functions $\mathbf{G}^\pm(z, t)$ along the line $t = 0$, which is the wave front, and along the line $t = 2(L - z)/c$. The jump discontinuities of $\mathbf{G}^\pm(z, t)$, are easily found by propagation of singularity arguments.

$$\mathbf{G}^+(z, 0) = \int_0^z \mathbf{A}(z') \, dz' + \frac{1}{2} (\mathbf{K}(z, 0) - \mathbf{K}(0, 0))$$

$$\left[\mathbf{G}^-(z, t) \right]_{t = \frac{2(L-z)}{c} - 0}^{t = \frac{2(L-z)}{c} + 0} = \frac{1}{4} e^{-\frac{1}{c} \int_z^L G(z', 0) \, dz'} \mathbf{G}(L, 0)$$

where the 2×2 matrix $\mathbf{A}(z)$ is given by (4.9).

For a homogeneous slab these jump discontinuities can be evaluated explicitly.

$$\mathbf{G}^+(z,0) = -z \left\{ \frac{1}{2c} \left(\mathbf{G}'(0) + 2\mathbf{K}'(0) \right) - \frac{1}{8c} \left(\mathbf{G}(0)\mathbf{G}(0) - 4\mathbf{K}(0)\mathbf{K}(0) \right) \right\}$$

$$\left[\mathbf{G}^-(z,t) \right]_{t=\frac{2(L-z)}{c}-0}^{t=\frac{2(L-z)}{c}+0} = \frac{1}{4} e^{-\frac{G(0)(L-z)}{c}} \mathbf{G}(0)$$

The Green functions equations, given by (7.3) and (7.4), can be solved numerically and the solutions $\mathbf{G}^\pm$ can be used to calculate the physical reflection and transmission kernels of the slab. Since they do not contain any double convolutions, as the imbedding equations do, these equations are in general one order faster to solve, but they require more memory space. Some computations are presented in the next section.
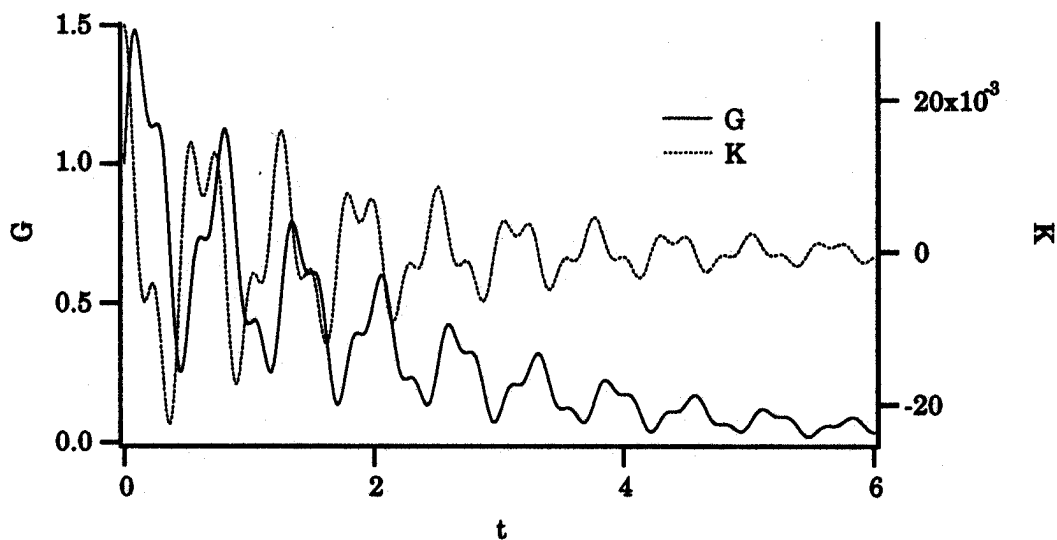
8   Numerical computations

Figure 8:   The susceptibility kernels for a multi-frequency Debye-Lorentz medium. The time scale is in units of L/c and the amplitude of the kernels in units of c/L.

Some numerical illustrations are given in this section. Numerical computations have been performed with both the invariant imbedding equations and the Green functions equations. The Green functions approach generates a numerical algorithm that is one order faster than the code based upon the imbedding approach. However, the Green functions approach is more memory consuming since all arrays have to be stored in the computations. In the imbedding approach old arrays can be discarded. Both methods give results with excellent accuracy.

The first example is a multi-frequency Lorentz medium. The analytic forms of the kernels are

$$G(t) = 8e^{-.2t} \sin 5t + 4e^{-.5t} \sin 10t + 2e^{-.5t} \sin 25t$$
$$K(t) = .02e^{-.5t} \cos 10t + .01e^{-.5t} \cos 25t$$

Notice that the same resonance frequencies that appear in $K(t)$ also appear in $G(t)$. The susceptibility kernel $G(t)$ has also an additional resonance that can be interpreted as a resonance from the non-chiral host material. The time is given in units of L/c and all frequencies in units of c/L. Notice also that $K(0) \neq 0$, so there is a rotation of the wave front. Figure 5 shows these kernels for three round trips in the medium, $0 \leq t \leq 6$. In Figure 6 the physical co-polarized kernel R_{co} is shown. The transmission kernels T_{co} and T_{cross} for this medium are shown in Figure 7.

An additional numerical example with a medium in which $G(0) \neq 0$ is the following combined Debye-Lorentz medium.

$$G(t) = e^{-t/2} + .5e^{-.5t} \sin 10t + .2e^{-.5t} \sin 25t$$
$$K(t) = .02e^{-.5t} \cos 10t + .01e^{-.5t} \cos 25t$$

Again the time is given in units of L/c and all frequencies in units of c/L. In Figures 8–10 the susceptibility kernels, reflection and transmission kernels are shown for three round trips in the medium, $0 \leq t \leq 6$. Notice that $R_{\mathrm{co}}(t)$ has a jump discontinuity at one round trip, $t = 2$, in the medium, due to the fact that $G(0) \neq 0$.
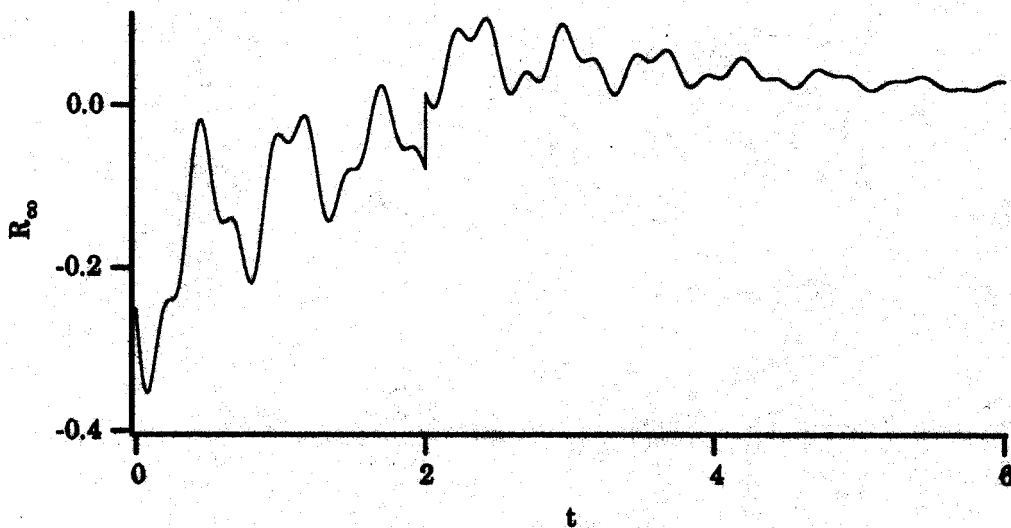

Figure 9: The reflection kernel $R_{\mathrm{co}}(t)$ for the multi-frequency Debye-Lorentz medium shown in Figure 8. The time scale is in units of L/c and the amplitude of the kernel in units of c/L.
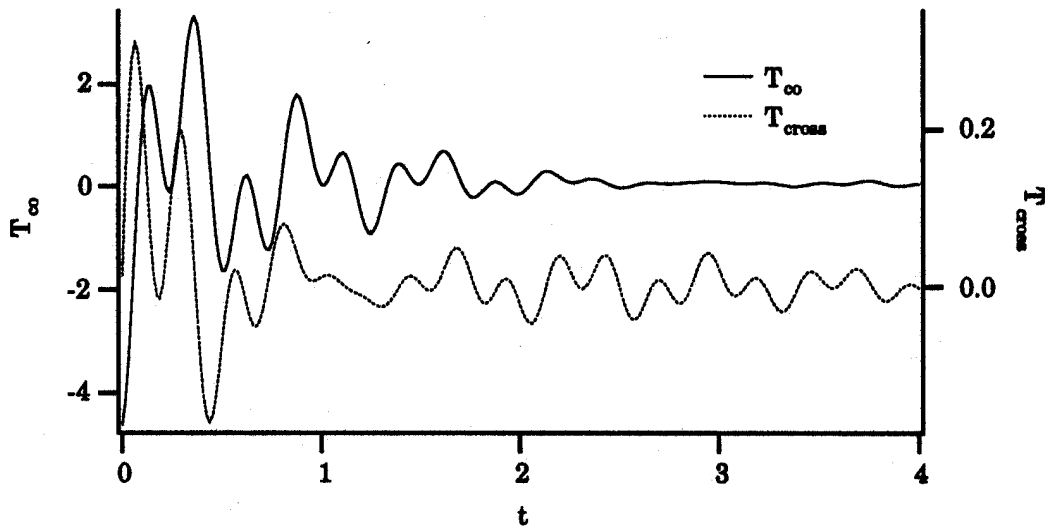
Figure 10:   The transmission kernels $T_{co}(t)$ and $T_{cross}(t)$ for the multi-frequency Debye-Lorentz medium shown in Figure 8. The time scale is in units of L/c and the amplitude of the kernel in units of c/L.

9 Conclusions

This paper gives a generalization of the analysis presented in Ref. [1] to a finite slab that has bi-isotropic properties. A generalization of the constitutive relations to cope with bi-isotropic effects in the time domain is used. Two methods, both based upon a wave splitting technique, are derived. The first uses an invariant imbedding procedure and the integro-differential equations for the reflection and transmission kernels are derived. These kernels are connected to the physical ones by employing the boundary conditions at both ends of the slab. A second method, which uses a Green functions approach, is also analysed. Numerical computations that illustrate both methods are given.

References

[1] R. S. Beezley and R. J. Krueger. An electromagnetic inverse problem for dispersive media. *J. Math. Phys.*, **26**(2), 317–325, 1985.

[2] R. Courant and D. Hilbert. *Methods of Mathematical Physics*, volume 2. Interscience Publishers, New York, 1962.

[3] N. Engheta and D. L. Jaggard. Electromagnetic chirality and its applications. *IEEE Antennas and Propagation Society Newsletter*, pages 6–12, October 1988.

[4] N. Engheta and P. G. Zablocky. A step towards determining transient response of chiral materials: Kramers-Kronig relations for chiral parameters. *Electronics Letters*, **26**(25), 2132–2133, 1990.

[5] A. Karlsson and G. Kristensson. Constitutive relations, dissipation and reciprocity for the Maxwell equations in the time domain. Technical Report LUTEDX/(TEAT-7005)/1–35/(1989), Lund Institute of Technology, Department of Electromagnetic Theory, P.O. Box 118, S-211 00 Lund, Sweden, 1989. Short published version *J. Electro. Waves Applic.*, **6**(5/6), 537–551 (1992).

[6] J. A. Kong. *Electromagnetic Wave Theory*. John Wiley & Sons, New York, 1986.

[7] G. Kristensson. Direct and inverse scattering problems in dispersive media— Green's functions and invariant imbedding techniques. In R. Kleinman, R. Kress, and E. Martensen, editors, *Direct and Inverse Boundary Value Problems*, Methoden und Verfahren der Mathematischen Physik, Band 37, pages 105–119, Frankfurt am Main, 1991. Peter Lang.

[8] G. Kristensson and R. J. Krueger. Direct and inverse scattering in the time domain for a dissipative wave equation. Part 1: Scattering operators. *J. Math. Phys.*, **27**(6), 1667–1682, 1986.

[9] G. Kristensson and R. J. Krueger. Direct and inverse scattering in the time domain for a dissipative wave equation. Part 2: Simultaneous reconstruction of dissipation and phase velocity profiles. *J. Math. Phys.*, **27**(6), 1683–1693, 1986.

[10] G. Kristensson and R. J. Krueger. Direct and inverse scattering in the time domain for a dissipative wave equation. Part 3: Scattering operators in the presence of a phase velocity mismatch. *J. Math. Phys.*, **28**(2), 360–370, 1987.

[11] G. Kristensson and R. J. Krueger. Direct and inverse scattering in the time domain for a dissipative wave equation. Part 4: Use of phase velocity mismatches to simplify inversions. *Inverse Problems*, **5**(3), 375–388, 1989.

[12] A. Lakhtakia. Recent contributions to classical electromagnetic theory of chiral media: what next? *Speculations in Science and Technology*, **14**(1), 2–17, 1991.

[13] I. V. Lindell and A. Viitanen. Green dyadic for the general bi-isotropic (non-reciprocal chiral) medium. Technical Report 72, Electromagnetics Laboratory, Helsinki University of Technology, FIN-02150 Espoo, Finland, 1990.